Biophys. Struct. Mechanism 3, 239–257 (1977)

Biophysics
of Structure
and Mechanism

Application of Radiationless Energy Transfer for Distance Measurements Across Membranes

Transition Probabilities for Radiationless Energy Transfer within Several Assemblies of Donors and Acceptors at Stationary Distances

L. Kampmann

Max-Planck-Insitut für Biophysik,
Kennedy-Allee 70, D-6000 Frankfurt (Main), Federal Republic of Germany

Abstract. For several 2- or 3-dimensional configurations of stationary donors and acceptors on or near a spherical membrane shell the transition probabilities for radiationless energy transfer are calculated, using Förster's approximation obtained for Coulombic dipole-dipole interaction of the transition moments. It turns out that the difference in the refractive indices for membrane (lipid) and bulk phase (water) has only a small influence on the transition probabilities. Furthermore, the curvature of biological cell surfaces can be neglected, but affects the energy transfer across small vesicles. The ratio thickness/radius of small vesicles can be determined by measuring fluorescence quenching of excited donors by acceptors on the other side of the membrane.

Key words: Energy transfer – Distance – Orientation factor – Membrane curvature – Refractive index.

1. Introduction

Fluorescent labels have been widely accepted as probes in membrane research. Changes in fluorescence intensity and shift of the band maximum have been discussed as measures for parameters such as polarity, electrical potential, conformation, viscosity or pH (Azzi, 1975).

A further valuable, but more complex technique is the measurement of fluorescence quenching of a donor by radiationless energy transfer to an acceptor: Although it takes some effort to find a proper donor-acceptor pair of labels and to determine the quantum yield of a donor after correction of the measured spectrum for fluorometer sensitivity and instrumental artefacts, there is a good chance – after some calculations – to come up with an elementary parameter: the distance between donor and acceptor(s).

The following report is an attempt to find the quantitative relations between the measurable parameter "fluorescence quenching" and a typical donor-acceptor distance for a set of various different geometrical assemblies of the fluorescent species on membrane surfaces. The following cases are considered:

A molecule S in an excited electronic state (denoted by *) can be deactivated by Coulombic interaction with a different molecule A in its vicinity or by luminescence. (Other deexcitation processes are assumed to be of minor importance compared to luminescence.) The probability of radiationless energy transfer by Coulombic interaction grows as the distance between donor S^* and acceptor A decreases. The amount of luminescence quenching is a measure of the distance S–A.

The following is a collection of calculations of transition probabilities for several geometrical configurations of the optically active species. In experiments being run these transition probabilities together with measurements of fluorescence quenching are used to determine distances on or across a biological membrane. The examples given below exclude donor self-transfer and are restricted to systems where donors and acceptors are near or fixed to a membrane. Both species are usually aromatic residues which are part of larger molecules, and their Brownian rotation is assumed to achieve complete averaging within the life time of the transfer process. Furthermore, the donor-acceptor distance is assumed to be large compared to distance changes during this life time.

The transition probability $n_{SA}dt$ for radiationless singlet-singlet energy transfer in solution from an excited donor S^* to an acceptor A within the time interval dt is given by

$$n_{SA} = t_S^{-1} \cdot (R_0/r)^6, \tag{1}$$

with[1]

$$R_0^6 = \frac{9000 \ln 10}{128\,\pi^5} \cdot \frac{k^2 Q_S}{n^4 N_L} \cdot \frac{\int F_S(\tilde{\nu})\, e_A(\tilde{\nu}) \tilde{\nu}^{-4} d\tilde{\nu}}{\int F_S(\tilde{\nu})\, d\tilde{\nu}}. \tag{2}$$

---

[1] If not denoted explicitly, all integrals have to be extended from 0 to infinity

t_S and Q_S are the true fluorescence life time and the quantum yield of S^* in absence of A, r the actual distance between donor and acceptor and R_0 the critical transfer distance for stationary molecules at which radiationless energy transfer and S^* deexcitation by fluorescence (or any other means) are of equal probability. Furthermore, n is the solvent refractive index, $F_S(\tilde{\nu})$ the fluorescence spectrum of the donor in arbitrary units, $e_A(\tilde{\nu})$ the decadic molar extinction of the acceptor, $\tilde{\nu}$ the wave number and k an orientation factor.

$$k = \cos \varphi_{SA} - 3 \cos \varphi_S \cos \varphi_A \,, \tag{3}$$

where φ_{SA} is the angle between the transition moment vectors $S^* \to S$ and $A \to A^*$, and φ_S and φ_A are the angles between these vectors and the directions $S \to A$. The relations (1), (2) were derived by Förster (1946, 1948, 1949) and are valid as long as the total electrostatic interaction between S^* and A is essentially dipole-dipole interaction between the transition moments.

If the fluorescence life time t_S is not measured directly, it is generally assumed that the relation

$$t_S^{-1} = \frac{8000\,\pi \ln 10}{c^2 N_L} \cdot \frac{n_F^3}{n_A} \cdot \int e_S(\nu)\nu^{-1}\, d\nu \cdot \frac{\int F_S(\nu)\, d\nu}{\int F_S(\nu)\nu^{-3}\, d\nu} \tag{4}$$

established by Birks and Dyson (1963), gives the most reliable values. Here ν = frequency; c = light velocity; n_F, n_A = refractive indices of the solutions in which the donor's fluorescence and extinction, respectively, was determined.

2. Transition Probabilities for Radiationless Energy Transfer for Donors and Acceptors on Different Sides of the Membrane

To make use of relation (2), the acceptor extinction curve $e_A(\tilde{\nu})$ and the donor fluorescence spectrum $F_S(\tilde{\nu})$ have to be measured, which may be done in bulk solutions. Not only the overlapping part, $e_A(\tilde{\nu})F_S(\tilde{\nu}) > 0$, of the curves, but also the fluorescence spectrum in its whole range has to be measured, since the quantum yield is proportional to $\int F_S(\tilde{\nu})\, d\tilde{\nu}$, (2) then yields R_0/k^2. If the system consists of only a single donor-acceptor pair, relation (3) together with R_0/k^2 gives the critical radius R_0. Otherwise the total transition probability is the sum of the probabilities of all possible pairs, where k may be different for each pair. Nevertheless can a critical distance be defined for that case also and is known after the total transition probability has been calculated. Together with the measurement of fluorescence quenching an unknown distance can now be determined, as is presented quantitatively in Section 3.

For several orientations of the transition moments the transition probabilities for acceptors and a donor on different sides of a flat membrane have been calculated by Drexhage et al. (1963). An additional case is given below. Furthermore, spherical membranes are taken into consideration, since in small vesicles the acceptors at any location on the membrane may contribute to radiationless energy transfer.

The averaged orientation factors computed below can be used for several purposes, such as the evaluation of energy transfer parallel to a membrane surface to find lateral distances, or for investigations on fluorescence depolarization. In this paper they represent the first step in finding the total transition probabilities for energy transfer across a membrane.

2.1. Spherical Membrane

2.1.1. Acceptors Fixed to Outer Membrane Surface

If donors S and acceptors A are distributed homogeneously on spherical membrane surfaces, donors inside, acceptors outside, the total transition probability $N_{SA}dt$ for radiationless energy transfer for one S^* to all A's during time interval dt is given by

$$N_{SA} = C \sum_{\substack{\text{all} \\ \text{pairs}}} \frac{k^2}{r^6} = C\, c_s N_L \cdot \int_{\substack{\text{outer} \\ \text{surface}}} \frac{k^2}{r^6}\, df \tag{5}$$

with r = distance S—A, df = surface differential and $C = R_0^6/k^2/t_S$, a constant independent of k according to (1), (2). The sum has to be extended over all S—A pairs, and the integral assumes a continuous (molar) surface concentration c_s of acceptors. If D and R are membrane thickness and radius, Figure 1 gives together with

$$r^2 = D^2 + 2h(R - D) \quad \text{and} \quad df/dh = 2\pi R \tag{6}$$

$$N_{SA} = 2\pi R c_s N_L C \int_0^{2R} \frac{k^2 dh}{(D^2 + 2h(R - D))^3} \tag{7}$$

2.1.1.1. In case all transition moments are normal to the cell surfaces

$$\cos\varphi_{SA} = (R - h)/R\,; \quad \cos\varphi_S = (D - h)/r\,;$$

$$\cos\varphi_A = (r^2 + R^2 - (R - D)^2)/(2rR)\,. \tag{8}$$

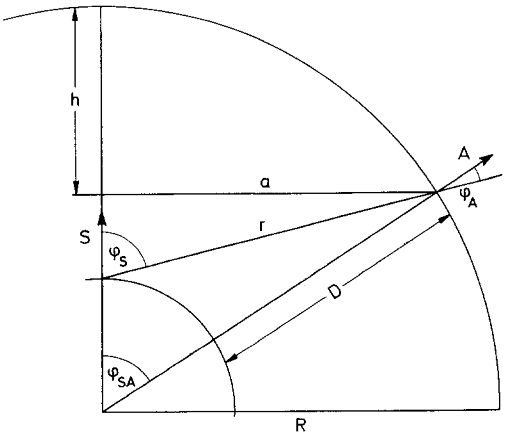

Fig. 1. Transition moments of donor S and acceptors A both vertical to membrane surface

From (3) and (7) follows with $d = D/R$ and $z = h/R$

$$N_{SA} = \frac{2\pi c_s N_L C}{D^4} \int_0^2 \frac{\left[\left(1 - z - \frac{3(d-z)(z(1-d)+d)}{d^2 + 2z(1-d)}\right) d^2\right]^2}{[d^2 + 2z(1-d)]^3} dz \,. \tag{9}$$

The d dependent integral term in (9) is listed in the following Table 1 and plotted in Figure 8, since its algebraic form is a bulky expression.

Table 1.

d	Integral in (9)	d	Integral in (9)
0	0.375 = 3/8	0.55	0.77013
0.05	0.39457	0.60	0.84666
0.10	0.41592	0.65	0.93850
0.15	0.43933	0.70	1.05003
0.20	0.46515	0.75	1.18711
0.25	0.49383	0.80	1.35767
0.30	0.52592	0.85	1.57257
0.35	0.56211	0.90	1.84684
0.40	0.60331	0.95	2.20155
0.45	0.65066	1	2.66667 = 8/3
0.50	0.70563		

For $d = 1$ the donor is located in the shell center, and the integral becomes 8/3. This case would be verified if the donor is located in the center of a globular protein and all acceptors fixed to its (spherical) surface. For a thin membrane the integral has a value of 3/8, i.e. the transition probability approaches Drexhage's value calculated for a flat membrane:

$$N_{SA}(d = 0) = \frac{3\pi c_s N_L C}{4\, D^4} \,. \tag{10}$$

2.1.1.2. In case the transition moments are random distributed in space, $k^2 = 2/3$ according to Förster (1951), i.e. k does not depend on df. After integration and incorporation of d (7) gives

$$N_{SA} = \frac{8\pi}{3} \cdot \frac{c_s N_L C}{D^4} \cdot \frac{d^2 + 2(1-d)}{[d^2 + 4(1-d)]^2} \,, \tag{11}$$

with the limiting cases $N_{SA}(d = 1) = (8/3)\pi\; c_s N_L C/D^4$ and

$$N_{SA}\;(d = 0) = (\pi/3) c_s N_L C/D^4 \,, \tag{12}$$

the latter again in concordance with Drexhage's calculation for a flat membrane.

2.1.1.3. If the configuration of donor and acceptors is maintained as in the former case, but all transition moments are allowed to rotate freely in the tangential planes

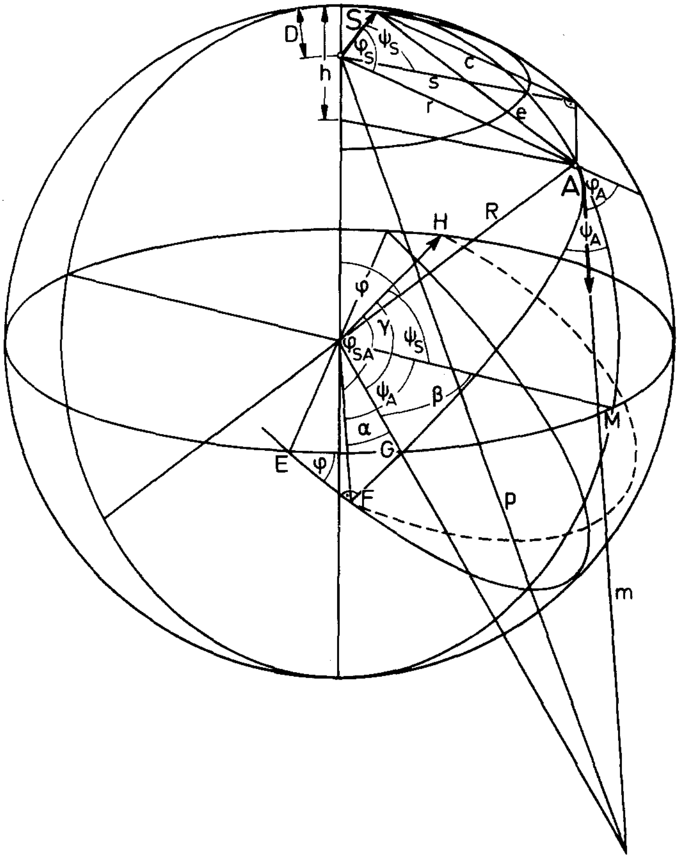

Fig. 2. All transition moments freely rotating in planes tangential to the membrane surfaces

holding the chromophores, the square of orientation factor k has to be averaged over both random angles prior to integration over the shell surface. With (6) and Figure 2

$$(h-D)^2+c^2=e^2=r^2+s^2-2rs\cos\varphi_S$$

and

$$\cos\varphi_S=(z(2-z)/(d^2+2z(1-d)))^{1/2}\cos\psi_S\,. \tag{13}$$

The spherical triangles EFG and FGH yield

$$\tan\beta=\cos\varphi\tan\psi_A\,;\quad \sin\alpha=\cos\beta\sin\varphi\,;\quad \cos\alpha=\sin\beta/\sin\psi_A\,;$$
$$\cos\varphi_{SA}=\cos\alpha\cos(\psi_S+\beta)-\sin\alpha\sin(\psi_S+\beta)\sin\psi_A\sin\varphi\,.$$

With the abbreviation $W=(1-z)\tan\psi_A$ follows

$$\cos\varphi_{SA}=\frac{W(\cos\psi_S-W\sin\psi_S)/\sin\psi_A-z(2-z)\sin\psi_A\,(\sin\psi_S+W\cos\psi_S}{1+W^2}. \tag{14}$$

From triangle AGM:

$$\cos \gamma = \sin \varphi \cos \beta \quad \text{or} \quad 1/\tan \gamma = \tan \varphi \cos \psi_A .$$

Together with $\tan \gamma = l/R$ and

$$r^2 + l^2 + 2rl \cos \varphi_A = p^2 = (R - D)^2 + R^2 + l^2 ,$$

$$\cos \varphi_A = (1 - d)\,(z(2 - z)/(d^2 + 2z(1 - d))^{1/2} \cos \psi_A \tag{15}$$

is obtained. (13), (14), (15) and (3) allow to compute the average value of k^2. After integration over ψ_S

$$k^2 = \frac{1}{4\pi} \int_0^{2\pi} \left[\frac{((1 - z)/\cos \psi_A)^2 + (z(2 - z) \sin \psi_A)^2}{1 + W^2} + \frac{9z(2 - z) \cos^2 \varphi_A}{d^2 + 2z(1 - d)} + \right.$$
$$\left. - 6 \left(\frac{z(2 - z)}{d^2 + 2z(1 - d)} \right)^{1/2} \cdot \frac{(1/\sin \psi_A - z(2 - z) \sin \psi_A)\, W \cos \varphi_A}{1 + W^2} \right] d\psi_A . \tag{16}$$

Elementary integrations for $z = 0$, $z = 1$, $z = 2$, and introduction of the complex variable $z = \exp(i\psi_A)$, which means integration over the unit circle in the complex plane, and applying the theorem of residuals, yield

$$\int_0^{2\pi} (1 + (1 - z)^2 \tan^2 \psi_A)^{-1}\, d\psi_A = 2\pi/(1 + |1 - z|) ;$$

$$\int_0^{2\pi} (1 - z)^2\, d\psi_A/(\cos^2 \psi_A(1 + (1 - z)^2 \tan^2 \psi_A)) = 2\pi |1 - z| ;$$

$$\int_0^{2\pi} \sin^2 \psi_A d\psi_A/(1 + (1 - z)^2 \tan^2 \psi_A) = \pi/(1 + |1 - z|)^2 \quad \text{for } 0 \le z \le 2, \tag{17}$$

where poles at $z_1, -z_1, z_2, -z_2$ with $z_1^2 = -z/(2 - z) = z_2^{-2}$ are the only singularities of the integrands in (17) within the unit circle. Hence, (16) leads to

$$k^2(z, d) = (1 + (1 - z)^2 + f(f - 2(1 - z))/4 , \tag{18}$$

with

$$f(z, d) = 3(1 - d)\, z\,(2 - z)/(d^2 + 2z(1 - d)) \tag{19}$$

(k^2 can also easily be expressed as a function of φ and d, since $\cos \varphi = 1 - z$.)

According to (7) the total transition probability from the donor to any acceptor on the outer surface is then given by

$$N_{SA} = \frac{\pi c_s N_L C}{2\, D^4} \int_0^2 \frac{1 + (1 - z)^2 + f(f - 2(1 - z))}{(d^2 + 2z(1 - d))^3}\, d^4 dz , \tag{20}$$

with f from (19) and relative membrane thickness $d = D/R$.

Since the integral's algebraic solution is a bulky expression, as it was in the first case above, it is plotted in Figure 8 as curve (20) and listed in the following Table 2.

Table 2.

d	Integral in (20)	d	Integral in (20)
0	0.09375 = 3/32	0.55	0.19253
0.05	0.09864	0.60	0.21166
0.10	0.10398	0.65	0.23463
0.15	0.10983	0.70	0.26251
0.20	0.11629	0.75	0.29678
0.25	0.12346	0.80	0.33942
0.30	0.13148	0.85	0.39314
0.35	0.14053	0.90	0.46171
0.40	0.15083	0.95	0.55039
0.45	0.16267	1	0.66667 = 2/3
0.50	0.17641		

For a flat membrane, $d \to 0$, (20) becomes

$$N_{SA}(d=0) = \frac{3\pi c_s N_L C}{16\, D^4}\,, \tag{21}$$

which is also consistent with Drexhage's value.

2.1.2. Donors Fixed to Membrane, Acceptors in Bulk Phase

2.1.2.1. Let a donor be fixed to the outer membrane surface with its transition moment freely rotating parallel to the membrane surface, and acceptors inside the shell with concentration c_A in bulk solution and their transition moments freely rotating in space. From spherical triangle FGH in Figure 3 follows

$$\cos \varphi_{SA} = \cos(\psi_A - \psi_S) \cos \beta\,. \tag{22}$$

Since p, h, m, e, a belong to the same plane,

$$\cos \gamma = -p/\mathrm{m}\,; \quad r^2 + r_A^2 - 2rr_A \cos \varphi_A = a^2 = p^2 + e^2 + h^2 + 2hp\,.$$

Substituting e^2 from triangle OLH' then gives

$$\cos \varphi_A = \sin \alpha \cos \psi_A \cos \beta - \cos \alpha \sin \beta\,. \tag{23}$$

Similarly with

$$r^2 + r_S^2 - 2rr_S \cos(\pi - \varphi_S) = b^2 = r^2 \cos^2 \alpha + (r \sin \alpha + r_S \cos \psi_S)^2$$
$$+ r_S^2 \sin^2 \psi_S\,;$$
$$\cos \varphi_S = \sin \alpha \cos \psi_S \tag{24}$$

Insertion of (22), (23), (24) into (3) and averaging over the angles ψ_S, ψ_A and β gives[2]

$$k^2(\alpha) = 1/3 + (1/2) \sin^2 \alpha \tag{25}$$

---

[2] Whereever k^2 appears, it represents the mean value after averaging over Brownian rotation of the transition moments during life time of the transition process. Whereas k is the unaveraged orientation factor defined by (3)

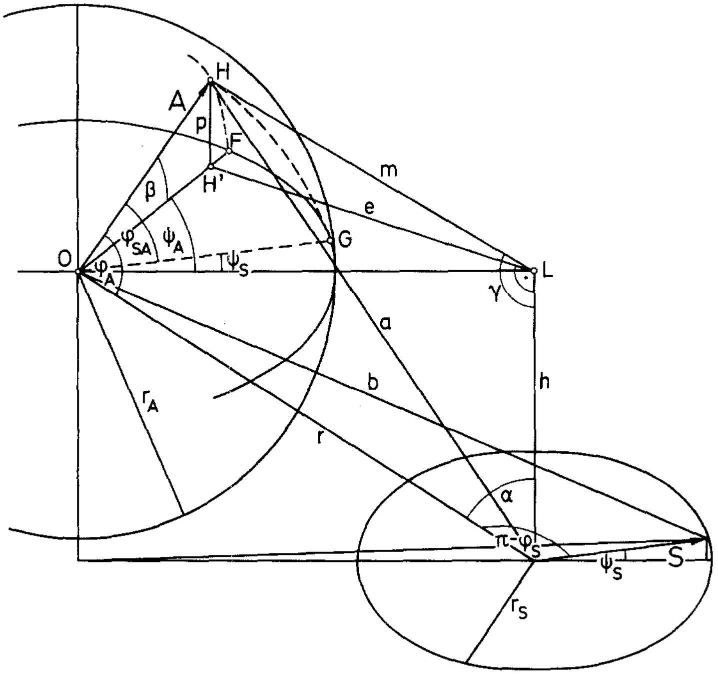

Fig. 3. Determination of orientation factor k with donor transition moment freely rotating in tangential plane and acceptor moments free in space

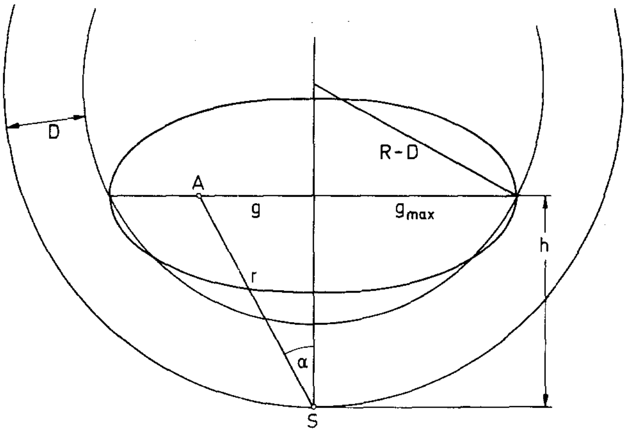

Fig. 4. Acceptors A in bulk phase, donor S fixed to membrane

To calculate the total transition probability $N_{SA}dt$, integration is first done over a thin slice of A's shown in Figure 4, then over all slices inside the sphere. With (5) (first relation), the volume element $dV = 2\,\pi\,g\,dg\,dh$ and elementary geometry from Figure 4

$$N_{SA} = CN_L c_A \int_{\substack{\text{interior}\\ \text{volume}}} k^2 r^{-6} dV$$

$$= 2\pi c_A N_L C \int_{h=D}^{2R-D} \int_{g=0}^{g_{\max}} \left(\frac{1}{3} + \frac{(1/2)g^2}{g^2 + h^2}\right) (g^2 + h^2)^{-3} g \, dg \, dh . \tag{26}$$

After integration

$$N_{SA} = \frac{\pi c_A N_L C}{12 D^3} \left[\frac{d^3}{2} \ln \left(\frac{2-d}{d}\right) + \frac{1-d}{(1-d/2)^3} \left(1 + \frac{d}{8}(d(14 + d(d-4)) - 20)\right)\right] \tag{27}$$

is received, where again $d = D/R$ is the relative membrane thickness. For a thin membrane the term holding the logarithm converges faster to 0 than d^2, so

$$N_{SA}(d \to 0) = \frac{\pi c_A N_L C}{12 D^3} (1 - 2d) . \tag{28}$$

As a check N_{SA} $(d = 0)$ was also derived directly, assuming an infinitely large flat membrane.

2.1.2.2.1. If the configuration from before is maintained, yet the donor transition moment is allowed to rotate freely in space, $k^2 = 2/3$, (26) has to be replaced by

$$N_{SA} = 2\pi c_A N_L C \int_{h=D}^{2R-D} \int_{g=0}^{g_{\max}} \frac{2}{3} (g^2 + h^2)^{-3} g \, dg \, dh . \tag{29}$$

Evaluation of (29) gives

$$N_{SA} = \frac{\pi c_A N_L C}{9 D^3} \left(\frac{1-d}{1-d/2}\right)^3 , \tag{30}$$

i.e. for a thin membrane

$$N_{SA}(d \to 0) = \frac{\pi c_A N_L C}{9 D^3} \left(1 - \frac{3d}{2}\right) . \tag{31}$$

2.1.2.2.2. In all cases with one species in bulk phase identity of the refractive indices in membrane phase, n_m, and bulk phase, n_b, was a tacit assumption. For a flat membrane – limiting case of (30) and (31) – this restriction is now skipped for a moment. Assuming that geometrical optics can still be applied, then follows from Figure 5

$$\frac{n_b}{n_m} = \frac{\sin \beta_m}{\sin \beta_b} = \frac{e/(D^2 + e^2)^{1/2}}{(g-e)/(a^2 + (g-e)^2)^{1/2}} \tag{32}$$

or

$$e = \frac{n_b}{n_m} (g - e)[(D^2 + e^2)/(a^2 + (g-e)^2)]^{1/2} , \tag{33}$$

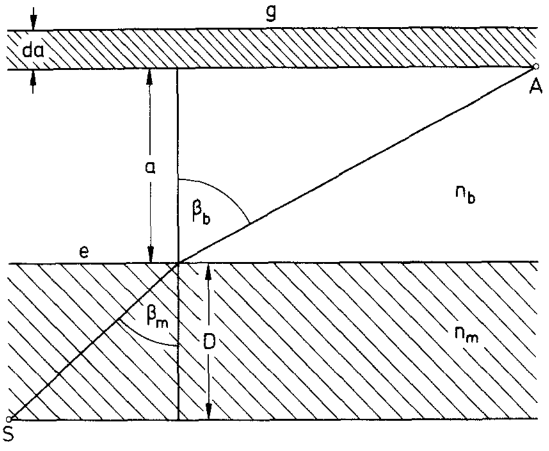

Fig. 5. Donor S fixed to (flat) membrane; acceptors A in bulk phase adjacent to other membrane side; refractive indices of membrane and bulk phase not necessarily identical

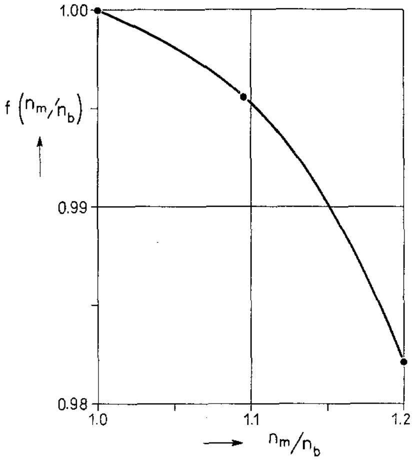

Fig. 6. Ratio $f = N_{SA}(n_m/n_b)/N_{SA}(n_m/n_b = 1)$ of transition probabilities versus n_m/n_b, the ratio of the refractive indices of membrane and bulk phase

where Snellius' law of light refraction is used. Solving the implicit Equation (33) for e for each given g and a, the optical pathway r for the current donor-acceptor pair is then, according to Figure 5

$$r = (D^2 + e^2)^{1/2} + (a^2 + (g - e)^2)^{1/2}. \tag{34}$$

The total transition rate is now

$$N_{SA} = c_A N_L C \int\int (2/3) r^{-6}\, 2\pi g \, dg \, da\,, \tag{35}$$

with r from (34) and e from (33). The numerical evaluation of (35) yields N_{SA} $(d = 0)$ as given by (31), but multiplied by a correction factor f, which depends only upon the ratio n_m/n_b. Figure 6, the plot of f versus n_m/n_b, shows that the transition probability obtained with the assumption $n_m = n_b$ is 0.5% too large for $n_m/n_b = 1.1$, the latter representing a realistic value for a biological membrane ($n_{\text{lipid}} = 1.46$; $n_{\text{water}} = 1.33$) (Seufert, 1970).

2.1.2.2.3. Although the application of geometric optics to dimensions below the wave length of light is not an exact procedure, the result of the calculations is assumed to be qualitatively correct. Above that it is generalized to any of the treated geometrical configurations of donors and acceptors: The transition probability for radiationless energy transfer calculated for biological membranes, assuming identical refractive indices for membrane and bulk phase, shows a negligibly small deviation from the exact value derived with the correct ratio of the refractive indices.

2.1.3. Donors and Acceptors in Bulk Phase

Let donors and acceptors be present in homogeneous solutions with the (molar) concentrations c_S and c_A separated by the membrane. All transition moments may rotate freely in space, i.e. $k^2 = 2/3$. Writing down the sum of the transition probabilities for a given A outside and all S's in a thin slice inside the membrane shell and vertical to the line OA, and then adding up over all slices gives with (5) and Figure 7

$$N_{SA}^{\mathrm{sum},\,A} = c_S N_L C \int_{h=0}^{2R'} \int_{g=0}^{g_{\max}} \frac{(2/3)\, 2\pi g\, dg}{(g^2 + (h + a)^2)^3}\, dh\,,$$

$$N_{SA}^{\mathrm{sum},\,A} = \frac{\pi}{3}\, c_S N_L C\, [(2(R' + a)(a^2 + 4R'(R' + a)))^{-1} - (3(a + 2R')^3)^{-1}$$

$$+ (3a^3)^{-1} - (2(R' + a)a^2)^{-1}]\,. \qquad (36)$$

The sum over all transition rates in a thin concentric shell da containing A's is then $c_A N_L d(\frac{4}{3}\pi(R' + a)^3)\, N_{SA}^{\mathrm{sum},\,A}$, hence for the sum of all transition rates for all S's to any A in the outer phase follows

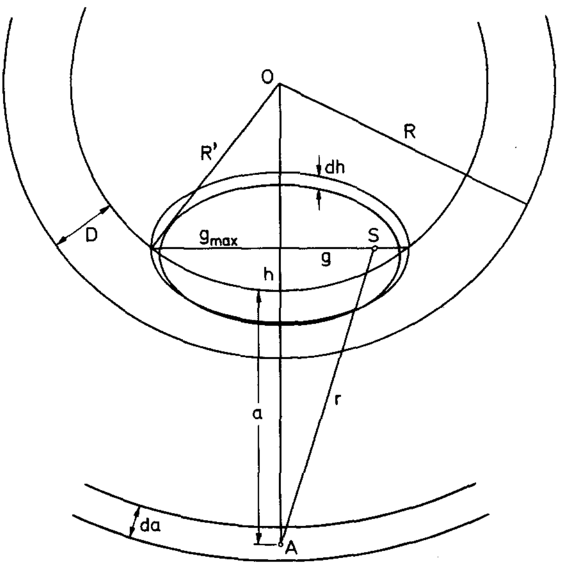

Fig. 7. Donors S and acceptors A both in bulk phases separated by a membrane

$$N_{SA}^{\text{sum}} = \frac{4}{3}\pi^2 c_S c_A N_L^2 C \int\limits_{a=d}^{\infty} (R' + a)^2 \, N_{SA}^{\text{sum},\,A} \, da \,. \tag{37}$$

Solving the integral and defining $d = D/R$ as before yields

$$N_{SA}^{\text{sum}} = \frac{2}{9}\pi^2 c_S c_A N_L^2 C \, \frac{1-d}{d^2} \left(1 + \frac{d + (1-d)/(2/d - 1)}{2/d - 1}\right). \tag{38}$$

The average rate for a single donor S inside the shell of transitions to any acceptor A outside is then

$$N_{SA}^{\text{av}} = \frac{\pi}{6} c_A N_L C \, \frac{d}{(1-d)^2} \left(1 + \frac{d + (1-d)/(2/d - 1)}{2/d - 1}\right). \tag{39}$$

After division of N_{SA}^{sum} by $(4/3)\,\pi\, R'^2$ follows for the sum of the transition probabilities of all donors to any acceptor, referred to membrane unit area,

$$N_{SA}^{\text{sum, area}} = \frac{\pi N_L^2 c_S c_A C}{18\, D^2} \left(1 + \frac{d + (1-d)/(2/d - 1)}{2/d - 1}\right), \tag{40}$$

which becomes for a flat membrane

$$N_{SA}^{\text{sum, area}}(d = 0) = \frac{\pi N_L^2 c_S c_A C}{18\, D^2}\,. \tag{41}$$

The last relation can easily be derived directly, starting from an infinitely large flat membrane.

2.1.4. Comparison of Transition Probabilities as Functions of Relative Membrane Thickness

Figure 8 allows a comparison of all transition probabilities calculated for different geometrical configurations and degrees of freedom of the transition moments. Ratios $N_{SA}(d)/N_{SA}(d = 0)$ are plotted versus relative membrane thickness $d = D/R$. (Numbers in Figure 8 reflect the corresponding equations.)

Although $N_{SA}(d)/N_{SA}(d = 0)$ approaches $d = 0$ with a nonvanishing gradient in all cases, this ratio can be seen to be close to 1 for biological cells, for which $d < 0.01$ is assumed. Consequently a smooth cell membrane can be treated as a flat membrane when computing the probabilities for radiationless energy transfer according to the Förster mechanism with donors and acceptors close to the membrane surfaces.

This is different for small vesicles, e.g. liposomes: d can go up to approximately 0.5, which means for the transition probabilities

Curve	(9)	(11)	(27)	(30)	(40)
N_{SA} $(d = 0.2)/N_{SA}$ $(d = 0)$	1.24	1.25	0.630	0.702	1.03
N_{SA} $(d = 0.5)/N_{SA}$ $(d = 0)$	1.88	1.98	0.226	0.296	1.22

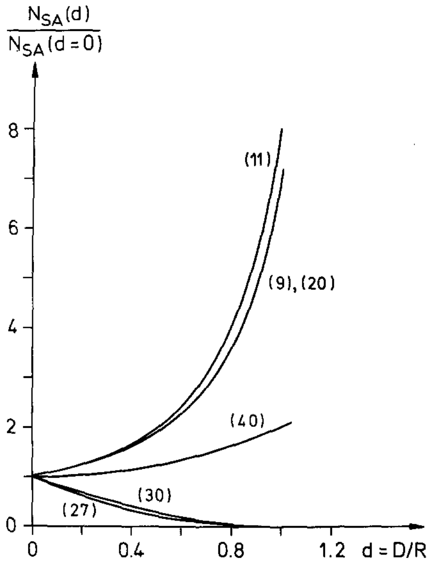

Fig. 8. Synopsis of the relative transition pobabilities as functions of relative membrane thickness for different geometries (numbers refer to corresponding equations)

Obviously the membrane curvature can now no longer be neglected, in other words: measuring the ratio of transition probabilities $N_{SA}(d)/N_{SA}(d = 0)$ is a procedure which yields the relative membrane thickness.

In order to determine the vesicle radius (if its membrane thickness is known) in an assembly of vesicles, using one of the relations given above, all of the following conditions have to be fulfilled:

1) The orientations of the donor and acceptor transition moments are known.

2) The vesicle size distribution is a single sharp peak.

3) All vesicles have a single shell only.

4) All vesicles are small enough to allow $N_{SA}(d)/N_{SA}(d = 0)$ to be experimentally significantly different from 1.

5) The surface concentration of acceptors is high enough, so that concentration fluctuations within a population of membranes have a negligible effect on the average total energy transfer rate of each donor.

6) The effect of light scattering is substracted.

In restriction 1) an approximate knowledge of the orientations may be sufficient, as is demonstrated by the small deviations within the curve pairs (9), (11) and (27), (30) in Figure 8. Restriction 5) is due to the strongly nonlinear dependence of energy transfer upon distance [relation (1)]. As an example, a system of two membranes with an average acceptor surface concentration of 15 chromophores per membrane, 10 on one and 20 on the other, will give an average total energy transfer rate for a donor inside each membrane, which is different from that of a system where both membranes hold 15 chromophores on their surfaces. In studies on dye labeling of protein surfaces this effect in case of low binding is known also (Gennis and Cantor, 1972).

2.2. Flat Membrane

2.2.1. Random Orientation of Transition Moments within Cones Normal to Membrane Surfaces

Thus far flat membranes appeared as limiting cases of spherical membranes. In the following the transition probability only for a flat membrane will be calculated, where donor and acceptors are fixed to its surfaces. But the restriction upon the transition moments will be more flexible now: Both moments shall rotate freely within cones, the axes of which are normal to the membrane, and their half opening angles ψ_S and ψ_A are parameters.

From the spherical triangles OSA', OBS and OBA' in Figure 9 follows

$$\begin{aligned}
\cos \varphi_{SA} &= \cos \alpha_S \cos \alpha_A + \sin \alpha_S \sin \alpha_A \cos (\beta_S - \beta_A)\,; \\
\cos \varphi_S &= \cos \alpha_S \sin \varphi + \sin \alpha_S \cos \varphi \cos \beta_S\,; \\
\cos \varphi_A &= \cos \alpha_A \sin \varphi + \sin \alpha_A \cos \varphi \cos \beta_A\,.
\end{aligned} \tag{42}$$

To determine the mean square of the orientation factor k, its square derived from (3) and relations (42) has to be averaged over the declination angles β_S and β_A and the inclination angles α_S and α_A, hence

$$\begin{aligned}
\overline{k^2} = {} & \int_{\alpha_S=0}^{\psi_S} \int_{\alpha_A=0}^{\psi_A} \int_{\beta_S=0}^{2\pi} \int_{\beta_A=0}^{2\pi} (\cos \varphi_{SA} - 3 \cos \varphi_S \cos \varphi_A)^2 \\
& \sin \alpha_S \sin \alpha_A \, d\beta_A \, d\beta_S \, d\alpha_A \, d\alpha_S / \\
& \left(4\pi^2 \int_{\alpha_S=0}^{\psi_S} \int_{\alpha_A=0}^{\psi_A} \sin \alpha_S \sin \alpha_A \, d\alpha_A \, d\alpha_S\right).
\end{aligned} \tag{43}$$

The fourfold integration results in the average value

$$\begin{aligned}
\overline{k^2}(\varphi, \psi_S, \psi_A) = {} & \tfrac{1}{9} (1 - 3 \sin^2 \varphi)^2 f(\psi_S) f(\psi_A) \\
& + \tfrac{1}{18} (1 - 3 \cos^2 \varphi (1 - \tfrac{3}{2} \cos^2 \varphi)) \; g(\psi_S)\, g(\psi_A) \\
& + \tfrac{1}{8} \sin^2 (2\varphi) \; (f(\psi_S)\, g(\psi_A) + g(\psi_S)\, f(\psi_A)),
\end{aligned} \tag{44}$$

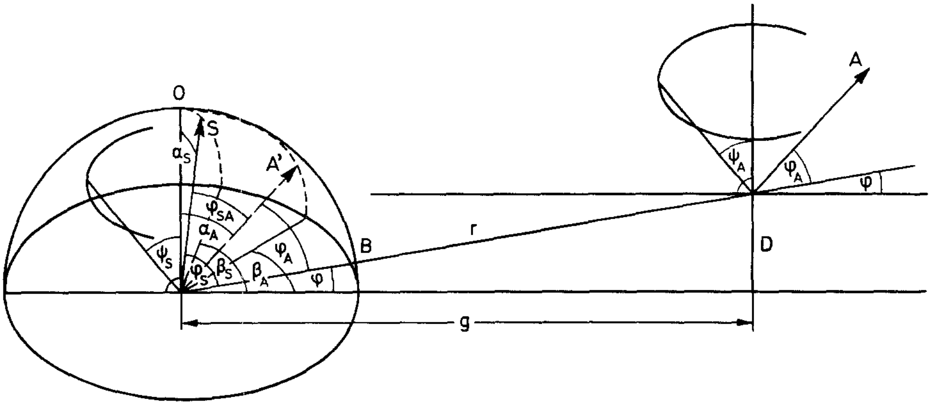

Fig. 9. Donor and acceptors fixed to different surfaces of a (flat) membrane; all transition moments rotating freely within cones, the axes of which are normal to the membrane

where per definition

$$f(\psi) = 1 + \cos\psi(1 + \cos\psi)\,; \quad g(\psi) = 2 - \cos\psi(1 + \cos\psi)\,.$$

Limiting cases of (44) are

$$k^2(\varphi, \psi_S = \psi_A = 0) = (1 - 3\sin^2\varphi)^2\,; \quad k^2(\varphi, \psi_S = \psi_A = \pi/2) = 2/3\,, \tag{45}$$

the latter value in concordance with Förster's value for both transition moments freely rotating in space.

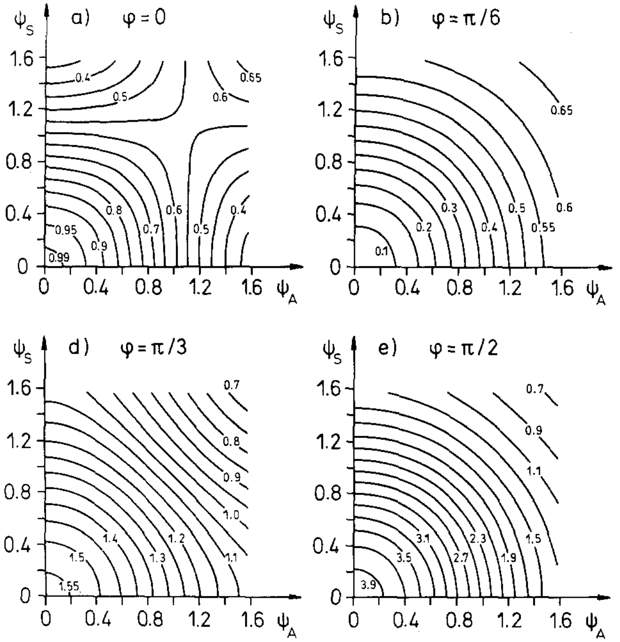

Fig. 10. Mean square of orientation factor k as function of elevation angle and cone half opening angles ψ_S and ψ_A (according to Fig. 9)

10a–10e. Constant levels of k^2 with φ as parameter

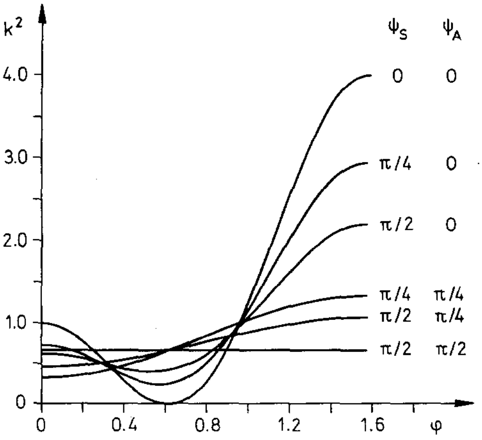

10f. k^2 versus φ with ψ_S and ψ_A as parameters

Figure 10f shows $k^2(\varphi)$, which is symmetrical in ψ_S and ψ_A, for all permutations, if both cone half opening angles step through 0, $\pi/4$ and $\pi/2$, whereas in Figures 10a–10e the two opening angles are plotted against each other, thus gaining constant levels of k^2 with angle φ increasing from one figure to the next. The limiting cases $\varphi = 0$ and $\varphi = \pi/2$, i.e. Figures 10a and 10e, were already presented by Eisinger and Dale (1974).

The transition probability for a donor to any acceptor on the other side of the membrane can now be determined from Figure 9 and relation (5), the latter applied to a flat membrane:

$$N_{SA} = c_s N_L C \int \frac{2\pi g\, k^2}{(g^2 + D^2)^3}\, dg \tag{46}$$

where the integral has to be extended over all acceptors with their surface concentration being c_s, and k^2 given in (44) with $\sin^2 \varphi = D^2/(g^2 + D^2)$. This leads to

$$\begin{aligned} N_{SA} &= \frac{\pi c_s N_L C}{3\, D^4} \left(1 + \tfrac{1}{4} \cos \psi_S (1 + \cos \psi_S)\right) \left(1 + \tfrac{1}{4} \cos \psi_A (1 + \cos \psi_A)\right) \\ &= \frac{\pi c_s N_L C}{3\, D^4}\, u(\psi_S, \psi_A)\,. \end{aligned} \tag{47}$$

Figure 11 shows $u(\psi_S, \psi_A) = u(\psi_A, \psi_S)$ with $\psi_S, \psi_A = 0, \pi/4, \pi/2$.

3. Relation between Membrane Thickness, Critical Distances and Fluorescence Quenching

In order to be able to use the transition probabilities calculated up to now for distance measurements, they have to be correlated to the critical distance R_0, derived for a single donor-acceptor pair.

A critical distance D_0 can be defined as the membrane thickness for which the transition probability for radiationless energy transfer from a donor to the acceptor

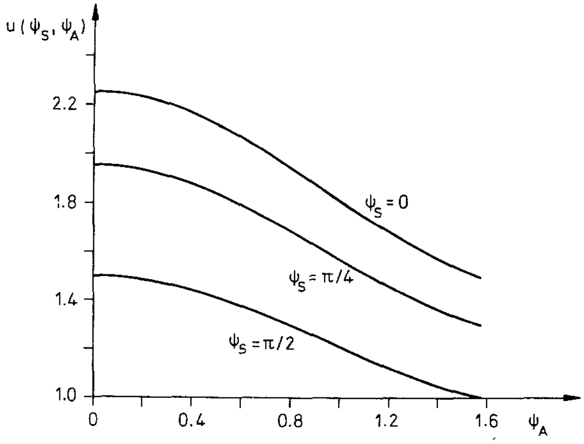

Fig. 11. Total transition probability (relative units) versus ψ_A (or ψ_S) with the other opening angle as parameter (orientation factor according to Fig. 9)

side of the membrane is equal to that of any other deactivation process of the donor. For the membrane thickness D_0 is now $N_{SA}dt = (1/t_S)dt$, hence according to Section 2

$$Cg/D_0^m = 1/t_S\,, \tag{48}$$

where g depends on basic constants and the geometry of the system, and m on the dimension of the donor and acceptor population, e.g. $m = 4$ for a transfer from surface to surface and $m = 3$ for surface to bulk phase. Together with the corresponding relation $C\,k^2/R_0^6 = 1/t_S$ for a single donor-acceptor pair with a distance R_0, the critical thickness is given by

$$D_0^m = gR_0^6/k^2 \tag{49}$$

where R_0^6/k^2 is independent of k^2 according to (2).

As has been pointed out already (for $m = 4$) by Drexhage, Zwick and Kuhn, the donor quantum yield Q_S (D) measured at a membrane thickness D is related to the quantum yield in absence of acceptors, $Q_S(\infty)$,by

$$Q_S(D)/Q_S(\infty) = 1/(1 + (D_0/D)^m) \tag{50}$$

hence with $Q_S(D)/Q_S(\infty)$ measured, R_0^6/k^2 determined via (2), and g deduced from Section 2, an unknown distance D is given by (49) and (50).

4. Concluding Remarks

In the preceding sections quantitative expressions have been derived which allow an experimental determination of distances on spherical or flat membranes. The influence of membrane curvature on fluorescence quenching turns out to be negligible for most of the biological membranes, i.e. the total transition probabilities for the limiting case of a flat membrane can be used. Yet for mitochondria membranes with a relative thickness d up to 0.2 the transition probability deviates by 20% or more from the value for a flat membrane, $d = 0$, depending on the geometrical conditions (table in Section 2.1.4.). On the other hand, for small lipid vesicles, like liposomes, d approaches 0.5, which in certain cases can be seen to change the total transition probability by more than 100% compared to its value for a flat membrane.

As an implication of Equation (1)–(4) only a limited distance range is available for energy transfer measurements. Outside this range Förster's dipole approximation of Coulombic interaction is invalid. At short distances multipole–multipole interactions are no longer negligible (Dexter, 1953), at a still smaller donor-acceptor separation "strong" interactions become predominant. Since the transition probability for radiationless energy transfer decreases with a high negative power of the chromophore distance, a greatest measurable distance of ca. $3D_0$ can be expected. Although 30–300 Å is a typical and experimentally verified distance range between chromophore layers (Kuhn and Möbius, 1971), relations (2) and (49) indicate that the critical distance D_0 depends strongly on the donor-acceptor spectral overlap and on the orientation factor k.

The model calculations given in the previous sections assume a sufficient knowledge about the rotational freedom of both chromophores and use this information to compute the mean square k^2 of the orientation factor. Usually the information derivable from stereochemical considerations is insufficient, i.e. gives only a rough range for k^2. If $k^2 = 2/3$, the average value for fast random rotation of both transition moments in space is taken, the uncertainty propagated to the distance to be determined is small if the true k^2 is in the range of ca. 0.4—4, but large if the true k^2 is close to 0 (according to (3) is $0 \leq k^2 \leq 4$). This can be seen from a plot of true k^2 against the ratio (distance assuming $k^2 = 2/3$)/(true distance).

Precise information about the orientation factor can be drawn from x-ray crystallographical investigations, but their significance shrinks considerately if extrapolation to a liquid system becomes necessary. Polarized fluorescence spectroscopy seems to be a more adequate technique in this respect: The measurement of depolarization during transfer can be used to estimate values of k^2 to an acceptably narrow range, as is discussed in detail by Dale and Eisinger (1975).

Acknowledgements. The author thanks Prof. Passow for interest and encouragement and Dr. Möbius for helpful suggestions.

Note added in proof.
The derived averaged orientation factors are also usable outside the context of this paper, e.g. in polarized fluorescence spectroscopy.

References

Azzi, A.: The application of fluorescent probes in membrane studies. Quart. Rev. Biophys. **8,** 237—316 (1975)

Birks, J. B., Dyson, D. J.: The relations between the fluorescence and absorption properties of organic molecules. Proc. Roy. Soc. A **275,** 135—148 (1963)

Dale, R. E., Eisinger, J.: Biochemical fluorescence concepts (eds. R. F. Chen, H. Edelhoch), pp. 115—284. New York: Marcel Dekker 1975

Dexter, D. L.: A theory of sensitized luminescence in solids. J. chem. Phys. **21,** 836—850 (1953)

Drexhage, K. H., Zwick, M. M., Kuhn, H.: Sensibilisierte Fluoreszenz nach strahlungslosem Energieübergang durch dünne Schichten. Z. Elektrochem. Bunsenges. physik. Chem. **67,** 62—67 (1963)

Eisinger, J., Dale, R. E.: Interpretation of intramolecular energy transfer experiments. J. molec. Biol. **84,** 643—647 (1974)

Förster, Th.: Energiewanderung und Fluoreszenz. Naturwissenschaften **33,** 166—175 (1946)

Förster, Th.: Zwischenmolekulare Energiewanderung und Fluoreszenz. Ann. Physik **2,** 55—75 (1948)

Förster, Th.: Experimentelle und theoretische Untersuchung des zwischenmolekularen Übergangs von Elektronenanregungsenergie. Z. Naturforsch. **4a,** 321—327 (1949)

Förster, Th.: Fluoreszenz organischer Verbindungen, p. 85. Göttingen: Vandenhoeck 1951

Gennis, R. B., Cantor, C. R.: Use of nonspecific dye labeling for singlet energy-transfer measurements in complex systems. A simple model. Biochemistry **11,** 2509—2517 (1972)

Kuhn, H., Möbius, D.: Systeme aus monomolekularen Schichten — Zusammenbau und physikalisch-chemisches Verhalten. Angew. Chem. **17/18,** 672—690 (1971)

Seufert, W. D.: Model membranes: Spherical shells bounded by one bimolecular layer of phospholipids. Biophysik **7,** 60—73 (1970)

Received May 4, 1976/Accepted February 11, 1977